

Part C: Beam-Columns

Beams

Basic Formulation

The Temporal Solution

The Spatial Solution

Rayleigh-Ritz Analysis

Rayleigh's Quotient

The Role of Initial Imperfections

An Alternative Approach

Higher Modes

Rotating Beams

Self-weight

A hanging beam

Experiments

Thermal Loading

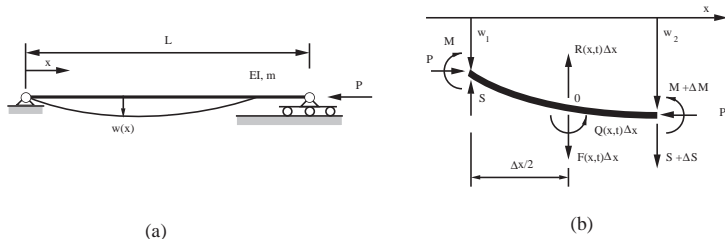
Beam on an Elastic Foundation

Elastically Restrained Supports

Beams with Variable Cross-section

A beam with a constant axial force

In this section we develop the governing equation of motion for a thin, elastic, prismatic beam subject to a constant axial force:



Beam schematic including an axial load.

It has mass per unit length m , constant flexural rigidity EI , and subject to an axial load P . The length is L , the coordinate along the beam is x , and the lateral (transverse) deflection is $w(x, t)$.

The governing equation is

$$EI \frac{\partial^4 w}{\partial x^4} + P \frac{\partial^2 w}{\partial x^2} + m \frac{\partial^2 w}{\partial t^2} = F(x, t). \quad (1)$$

This **linear partial differential equation** can be solved using standard methods.

We might expect the second-order ordinary differential equation in time to have oscillatory solutions (given positive values of flexural rigidity etc.), however, we anticipate the dependence of the form of the temporal solution will depend on the magnitude of the axial load.

The Temporal Solution

In order to be a little more specific, (before going on to consider the more general spatial response), let us suppose we have ends that are pinned (simply supported), i.e., the deflection (w) and bending moment ($\partial^2 w / \partial^2 x$) are zero at $x = 0$ and $x = l$. In the general case we would assume an exponential form for the solution but with these relatively convenient boundary conditions we can take:

$$w(x, t) = \sum_{n=1}^{\infty} Y(t) \sin \frac{n\pi x}{l}. \quad (2)$$

The **temporal part** of the solution can be obtained by assuming

$$Y_n(t) = A_n e^{i\omega_n t}, \quad (3)$$

and substituting into equation 1 leads to

$$\sum_{n=1}^{\infty} \left[\left[EI \frac{n^2 \pi^2}{l^2} - P \right] \frac{n^2 \pi^2}{l^2} - m\omega_n^2 \right] A_n \sin \frac{n\pi x}{l} e^{i\omega_n t} = 0. \quad (4)$$

Clearly the term in the outer square brackets must vanish for a generally valid solution so that

$$\omega_n^2 = \frac{n^4 EI \pi^4}{ml^4} \left[1 - \frac{Pl^2}{n^2 EI \pi^2} \right]. \quad (5)$$

If we define the following parameters:

$$P_{cr_n} = n^2 EI \pi^2 / l^2 \quad \bar{\omega}_n^2 = n^4 EI \pi^4 / ml^4, \quad (6)$$

equation 5 becomes

$$\omega_n = \pm \bar{\omega}_n \sqrt{1 - P/P_{cr_n}}, \quad (7)$$

and we see that the nature of the solution depends crucially on the discriminant. Making use of the Euler identities we shall consider four representative cases, where A_n and B_n are constants obtained from the initial conditions.

- ▶ If $P = 0$ then

$$Y_n(t) = A_n \cos \bar{\omega}_n t + B_n \sin \bar{\omega}_n t \quad (8)$$

and we observe simple harmonic motion, a familiar result from linear vibration theory.

- ▶ If $P < P_{cr_n}$ then

$$Y_n(t) = A_n \cos \omega_n t + B_n \sin \omega_n t, \quad (9)$$

where

$$\omega_n = \pm \bar{\omega}_n \sqrt{1 - P/P_{cr_n}}, \quad (10)$$

and simple harmonic motion results. Any perturbation will induce oscillatory motion about equilibrium. The response neither grows or decays.

- ▶ If $P = P_{cr_n}$ then the solution can be written as

$$Y_n(t) = A_n + B_n t, \quad (11)$$

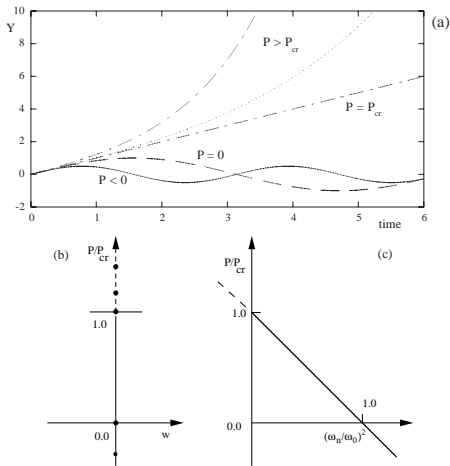
and the motion grows linearly with time (this is a **special** case with multiple roots).

- ▶ If $P > P_{cr_n}$ then

$$Y_n(t) = A_n \cosh \omega_n t + B_n \sinh \omega_n t, \quad (12)$$

and the motion grows exponentially with time.

Examples of these are shown (a) below in which the natural frequency in the absence of axial load was taken as unity. Also shown in this figure are the stability of equilibrium (b), and effective natural frequency (c), as a function of axial load.



(a) The lateral motion of the strut in terms of the first mode as a function of the axial load. (b) stability of equilibrium, (c) Frequency-axial load relationship.

Let's focus attention on the lowest natural frequency and its corresponding mode ($n = 1$). With no axial load ($P = 0$) we obtain $\omega_1 = \bar{\omega}_1$. However, as the axial load increases the natural frequency decreases according to equation 7, i.e., we observe a **linear relationship** between the magnitude of the axial load and the square of the natural frequency. Any non-zero initial conditions result in bounded motion, and we may consider this to be a stable situation (at least in the sense of Lyapunov).

When $P = P_{cr1}$, ω_1 vanishes and the solution becomes real (the linearly increasing (constant velocity) solution), and any inevitable perturbation will cause the system to become unstable. This type of instability is not oscillatory but rather monotonic since, locally, the deflections grow in one direction (determined by the initial conditions). This type of behavior is sometimes referred to as **divergence**. The higher modes ($n > 1$) will exhibit oscillations but the important practical information has been gained.

The Spatial Solution

For tensile axial loads the system does not suffer instability, and we shall see that the lowest natural frequency **increases** with tensile force (in similarity to the string).

Returning to equation 1 and focusing on the free vibration problem with an external but constant axial load ($F(x, t) = 0$) we can write a general solution to the spatial part of the solution by assuming $w(x, t) = W(x) \cos \omega t$ and we then have

$$EI \frac{d^4 W(x)}{dx^4} - P \frac{d^2 W(x)}{dx^2} - m\omega^2 W(x) = 0. \quad (13)$$

Introducing the non-dimensional beam coordinate $\zeta = x/l$ then we can write a general solution to the above equation in the form

$$W(\zeta l) = c_1 \sinh M\zeta + c_2 \cosh M\zeta + c_3 \sin N\zeta + c_4 \cos N\zeta, \quad (14)$$

in which M and N are give by

$$\begin{aligned} M &= \sqrt{\Lambda + \sqrt{\Lambda^2 + \Omega^2}} \\ N &= \sqrt{-\Lambda + \sqrt{\Lambda^2 + \Omega^2}} \end{aligned} \quad (15)$$

and using non-dimensionalized axial load and frequency:

$$\Lambda = Pl^2/(2EI) \quad \Omega^2 = m\omega^2 l^4/(EI). \quad (16)$$

We now apply the **boundary conditions**. We shall use clamped-pinned to make things a little more interesting. At the left hand end we have the fully clamped conditions

$$W(0) = 0 \quad \frac{dW(0)}{dx} = 0, \quad (17)$$

and pinned, or simply supported, at the right hand end:

$$W(l) = 0 \quad \frac{d^2W(l)}{dx^2} = 0. \quad (18)$$

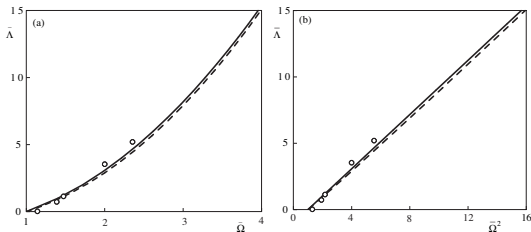
In fact, we assume that this support is a roller, i.e., it does not allow vertical displacement or resistance to bending moments. If the horizontal displacement is suppressed then **membrane effects** may induce additional axial loading - a feature to be explored in more detail later, and will prove to be an important consideration in the dynamic response of axially-loaded plates as well.

Plugging these boundary conditions into the general solution (equation 14) and applying the condition for non-trivial solutions (i.e., setting the determinant equal to zero) leads to the **characteristic equation**

$$M \cosh M \sin N - N \sinh M \cos N = 0. \quad (19)$$

This equation can be solved numerically by assuming Λ and solving for Ω or vice versa.

The figure below shows the lowest root of this equation as the solid line (normalized with respect to the natural frequency in the absence of axial load, i.e., $\bar{\Lambda} = \Lambda/\pi^2$). Plotting the square of the natural frequency (part b) gives almost, but not quite, a straight line. Only tensile loads (normalized by the Euler load) are plotted in this figure.



The relation between axial load and (a) frequency, (b) frequency squared for a clamped-pinned beam.

Also plotted in these figures (as a dashed line) is an upper bound based on the expression

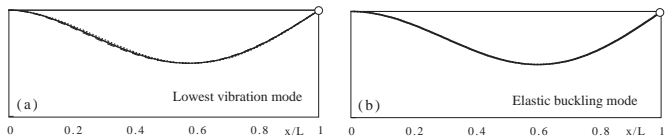
$$\Omega = \sqrt{1 + \gamma\Lambda}, \quad (20)$$

where $\gamma = 0.978$ for the clamped-pinned boundary conditions.

The corresponding **mode shape** comes from the smallest root of the characteristic equation given by equation 14 with the coefficients

$$c_1 = 1, \quad c_2 = -\tanh M, \quad c_3 = -M/N, \quad c_4 = (M/N) \tan N, \quad (21)$$

and is plotted in figure below with the modeshape normalized such that its maximum amplitude is unity.



The mode shapes corresponding to (a) the lowest natural frequency, and (b) the elastic critical load, for a clamped-pinned axially-loaded beam.

Although not apparent in the figure there are actually three curves plotted. Superimposed on the zero-load case (a continuous curve) is the mode shape when the beam is subject to a compressive load of one half the elastic critical load, which corresponds to $U = -5.55$ in the units used. Note that this has an almost negligible effect on the mode shape despite the frequency dropping from $\Omega_0 = 15.42$ for the unloaded case to $\Omega = 10.42$ (and indicated by a dotted line). Similarly a tensile force of this same magnitude causes the lowest natural frequency to increase to $\Omega = 19.09$ but has only a minor influence on the mode shape (dashed line). In general, despite the relatively strong effect of an axial load on the natural frequencies of thin beams (and strings), the effect on mode shapes is **relatively minor**. We shall see later that this is not necessarily the case for plated structures. Equation 19 of course is a **transcendental equation** and has an infinite number of roots. These correspond to higher modes and will be considered later.

Before leaving this section we briefly touch upon some simple experimental results.



A simple experimental set-up for a beam with clamped-pinned boundary conditions in a displacement-controlled testing machine.

Suppose we have a thin strip of polycarbonate material 44 mm wide by 1.52 mm thick with a length of 318 mm (as shown on the previous page). This material has a Young's modulus estimated at 2.4 GPa, a density of $1.142 \times 10^3 \text{ Kg/m}^3$ and boundary conditions such that it can be considered simply-supported at one end and fully clamped at the other. We would expect an elastic critical load in the vicinity of $P_{cr} = 20.2EI/L^2 \approx 6\text{N}$ (with the buckled mode shape is shown in part (c)). We would expect a fundamental natural frequency in the vicinity of $f_1 = 15.4/(2\pi)\sqrt{EI/(\rho AL^4)} \approx 15\text{Hz}$.

Using these two values to normalize the measured (tensile) axial loads and the measured fundamental frequencies we obtain the data points shown in the figure. Similar tests on struts of other lengths and thicknesses can also be suitably nondimensionalized and the results confirm the almost linear (stiffening) effect of the (tensile) loads on the square of the natural frequencies. It should be mentioned here that in a practical testing situation there is likely to be a little membrane effect due to finite amplitude oscillations as well as possible friction at the pinned end. This is especially the case when the axial loading is compressive.

Energy-based approximate analyses

In using conventional beam theory in a previous section, we made the standard assumption that the bending moment and curvature were linearly related (through the flexural rigidity EI). This allowed a relatively simple analytic solution to be found. However, a number of approximate techniques have been developed which are relatively easy to apply, can be used in somewhat more complicated situations including large deflections, e.g., in the post-buckled regime.

If we do **not** restrict ourselves to small deflections and curvatures it can be shown that the curvature ψ is related to the lateral deflection via

$$\psi = w''(1 - w'^2)^{-1/2}, \quad (22)$$

where the prime denotes differentiation with respect to the **arc length** x . It can be shown that this is roughly equivalent to the curvature expression more familiar from standard geometry. It can also be shown (based on inextensional beam theory) that the total strain energy stored in bending is

$$U = \frac{1}{2}EI \int_0^L \psi^2 dx. \quad (23)$$

Placing ψ in the above expression and expanding, we obtain

$$U = \frac{1}{2}EI \int_0^L \left(w''^2 + w''^2 w'^2 + \dots \right) dx. \quad (24)$$

Similarly, we can relate the end-shortening to the lateral deflection:

$$\xi = L - \int_0^L (1 - w'^2)^{1/2} dx, \quad (25)$$

which in turn leads to the potential energy of the load:

$$V_P = -\frac{1}{2}P \int_0^L \left(w'^2 + \frac{1}{4}w'^4 + \dots \right) dx. \quad (26)$$

Given a form for w these two expressions (24 and 26) can then be added to the appropriate kinetic energy expression.

We assume a solution (buckling mode) of the form

$$w = Q(t) \sin \frac{\pi X}{L}, \quad (27)$$

which can then be used to evaluate the strain and end-shortening energies to give

$$\begin{aligned} V(Q) = U + V_p = & \frac{1}{2}EI \left(\frac{\pi}{L}\right)^4 \frac{L}{2}Q^2 + \frac{1}{2}EI \left(\frac{\pi}{L}\right)^6 \frac{L}{8}Q^4 + \dots \\ & -P \left(\frac{1}{2} \left(\frac{\pi}{L}\right)^2 \frac{L}{2}Q^2 + \frac{1}{2} \left(\frac{\pi}{L}\right)^4 \frac{3L}{32}Q^4 + \dots \right), \end{aligned} \quad (28)$$

and a kinetic energy expression

$$T = \frac{1}{2}m \int_0^L \dot{w}^2 dx = \frac{1}{2}m \left(\frac{L}{2}\right) \dot{Q}^2. \quad (29)$$

where terms including the first nonlinear potential energy contribution have been retained. For example, if P is greater than the Euler critical value then the potential energy takes the form of two minima separated by a hill-top, i.e., a **twin-well** form of potential energy.

Non-trivial equilibrium paths ($dV/dQ = 0$) are now given by

$$\Lambda = 1 + \frac{\pi^2}{8} \left(\frac{Q}{L} \right)^2 \quad (30)$$

and again application of the general theory (i.e., $\omega^2 = V_{11}/T_{11}$) leads to

$$\frac{(d\Lambda/d\omega)_p}{(d\Lambda/d\omega)_f} = -2 \quad (31)$$

A similar (but less accurate) analysis can be based on assumed polynomial buckled and vibration mode shapes. For example, by assuming a simple parabola as the fundamental mode shape we would arrive at a natural frequency of 120 (as opposed to π^4) and a critical load of 12 (as opposed to π^2). That these values are higher than the exact values is typical for Rayleigh-Ritz analysis and is a consequence of the system being effectively constrained to take the assumed mode which therefore artificially stiffens the structure leading to higher values.

A useful means of estimating the fundamental frequency of vibration can be based on the fact that the frequency corresponds to a stationary value in the neighborhood of a natural mode. Using an assumed mode it can be shown that for an inexact eigenvector we get an eigenvalue that differs from the true value to the second order.

So far we have focused on directly **applied** axial loads, but there are a number of other ways in which **induced** axial loads occur. If the ends of the member are constrained in the axial direction then membrane effects can occur for deflections which are not especially large.

The period of motion for a given set of initial conditions can be obtained as a first integration. The energy contributions are

$$T = \frac{1}{2}m \int_0^L (\dot{w})^2 dx \quad (32)$$

$$U = \frac{1}{2}EI \int_0^L (w'')^2 dx \quad (33)$$

$$W = \frac{1}{2}P \int_0^L \frac{1}{2}(w')^2 dx, \quad (34)$$

in which it can be shown that the induced axial load is given by

$$P = \frac{EI}{2Lr^2} \int_0^L (w')^2 dx, \quad (35)$$

where for a beam of cross sectional area A , and radius of gyration r we have $I = Ar^2$.

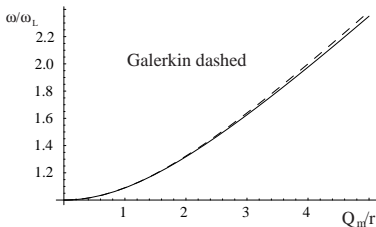
Suppose the ends are simply-supported (but not allowed to move in-plane), then the lowest mode for the linear problem is simply a half sine wave $w = Q(t) \sin(\pi x/L)$. We are primarily interested in the maximum amplitude of motion Q_m , then evaluating the energy terms and adding them we obtain the total energy constant

$$C = \frac{\pi^4 EI}{mL^4} Q_m^2 + \frac{\pi^4 EI}{8mL^4 r^2} Q_m^4, \quad (36)$$

which then can be used to obtain the phase trajectory as a function of the initial conditions (i.e., maximum amplitude). This can be subjected to separation of variables and integrated (numerically) to obtain the natural period (and hence frequency) as a function of maximum amplitude.

The frequency is normalized with respect to the (constant) linear natural frequency (ω_L). The result is shown below together with a Galerkin approach (the dashed line) which yields

$$\left[\frac{\omega}{\omega_L} \right]^2 = 1 + \frac{3}{16r^2} \left(\frac{Q_m}{r} \right)^2. \quad (37)$$



The increase in natural frequency with amplitude for a simply-supported strut which is constrained from moving axially at the ends (Wagner).

A similar approach can be used for clamped boundary conditions (which are a little more likely to include in-plane end restraint).

In cases in which appreciable axial loading is present and especially in buckling it is well established that small geometric imperfections may have a profound effect on behavior. In terms of the linear theory, consider a simply-supported strut with an initial deflection (i.e., prior to the application of any load) of the form $w_0 = Q_0 \sin(\pi x/L)$. In this case the static response is given by

$$w_{total} = w_0 + w = \left(\frac{Q_0}{1 - \alpha} \right) \sin(\pi x/L), \quad (38)$$

where $\alpha = P/P_E$ and P_E is the Euler load, and thus, the maximum lateral deflection (at the strut mid-point) is given by

$$Q_{max} = \frac{Q_0}{1 - \alpha} = \frac{Q_0}{1 - \frac{P}{P_E}}, \quad (39)$$

i.e., deflections grow unlimited when the elastic critical load for the underlying geometrically perfect strut is approached.

In terms of the large deflection theory the local form of the potential energy in the vicinity of a bifurcation is perturbed to:

$$V = \frac{1}{24} V_{1111}^c Q^4 + \frac{1}{2} V_{11}^{\prime c} Q^2 \lambda + \dot{V}_1^c \epsilon Q, \quad (40)$$

where ϵ is a small parameter (which breaks the symmetry). In the case of a slender strut this small parameter might relate to an initial curvature, axial load offset or small lateral load: they can be shown to have quite similar effects on subsequent behavior.

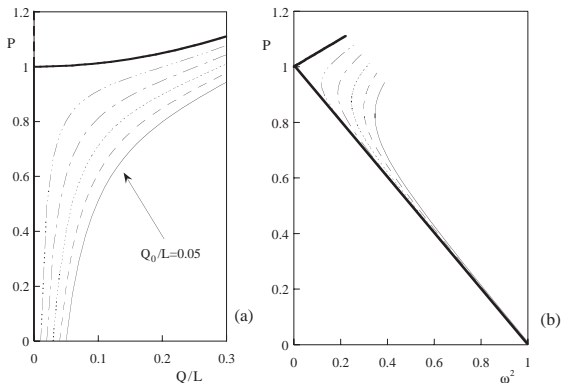
For the continuous strut (with a small initial deflected amplitude of Q_0 - representing a half sine wave) the equilibrium paths are given by

$$\Lambda = 1 + \frac{\pi^2}{8} \left(\frac{Q}{L}\right)^2 - \left(\frac{Q_0}{L}\right) \left(\frac{L}{Q}\right), \quad (41)$$

and the frequency expression is given by

$$\Omega^2 = 2(\Lambda - 1) + 3 \left(\frac{Q_0}{L}\right) \left(\frac{L}{Q}\right), \quad (42)$$

We see that these degenerate into the perfect case for $Q_0 = 0$.



(a) Equilibrium paths for a slightly curved axially loaded strut, (b) corresponding frequency-load relation.

We see that since there is no distinct instability the natural frequency simply reaches a minimum in the vicinity of the critical load for the underlying perfect system (a super-critical pitchfork bifurcation). The different dashes in this figure represent levels of initial imperfection incremented by 0.01 from 0 to 0.05.

In this section we conduct an alternative analysis of a simply supported strut. Here, we apply **Hamilton's principle** followed by a single mode Galerkin procedure. Again axial load is included in the analysis and moderately large deflections (corresponding to a degree of stretching) are allowed, i.e., we focus attention again on a system in which no displacement or rotation is allowed at the supports.

We state Hamilton's principle in the form

$$\int_{t_1}^{t_2} (\delta T - \delta U + \delta W) dt = 0 \quad (43)$$

The strain energy consists of bending and stretching terms:

$$\delta U = \int_0^L \left[N_x \delta \left(\frac{\partial u}{\partial x} \right) + N_x \frac{\partial w}{\partial x} \delta \left(\frac{\partial w}{\partial x} \right) + EI \left(\frac{\partial^2 w}{\partial x^2} \right) \delta \left(\frac{\partial^2 w}{\partial x^2} \right) \right] dx. \quad (44)$$

The kinetic energy is given by

$$\delta T = \int_0^L m \frac{\partial w}{\partial t} \delta \left(\frac{\partial w}{\partial t} \right) dx. \quad (45)$$

and the work done by the external load

$$\delta W = \int_0^L \left[P \delta \left(\frac{\partial u}{\partial x} \right) + P \frac{\partial w}{\partial x} \delta \left(\frac{\partial w}{\partial x} \right) \right] dx. \quad (46)$$

Integrating by parts, applying the boundary conditions (pinned supports at either end) leads to the equation of motion (in the lateral direction) of

$$m\ddot{w} + EI \frac{\partial^4 w}{\partial x^4} - \frac{\partial}{\partial x} \left[(N_x - P) \frac{\partial w}{\partial x} \right] = 0 \quad (47)$$

where the second term consists of axial effects from both the external applied load, P , and large deflections, i.e., coupling between bending and stretching, N_x , where N_x is based on a truncation of the end shortening and given by

$$N_x = \frac{EA}{2L} \int_0^L \left(\frac{\partial w}{\partial x} \right)^2 dx, \quad (48)$$

in which A is the cross-sectional area of the member.

The deflection w and distance along the beam x can be scaled in the usual way using

$$W = w/h \quad \xi = x/L \quad (49)$$

which enables equation 47 to be rewritten as

$$\frac{\partial^4 W}{\partial \xi^4} - \frac{12h}{EL^2} \left(\frac{L}{h}\right)^4 \frac{\partial}{\partial \xi} \left[(N_x - P) \frac{\partial W}{\partial \xi} \right] + \frac{12mh}{E} \left(\frac{L}{h}\right)^4 \frac{\partial^2 W}{\partial t^2} = 0. \quad (50)$$

We now scale the in-plane loads and time using,

$$p = P \left(\frac{L^2}{EI} \right) \quad (51)$$

$$N_\xi = N_x \left(\frac{L^2}{EIA} \right) \quad (52)$$

$$\tau = t \sqrt{\frac{EI}{mL^4}} \quad (53)$$

leading to the final nondimensional equation of motion

$$\frac{\partial^2 W}{\partial \tau^2} + \frac{\partial^4 W}{\partial \xi^4} - \frac{\partial}{\partial \xi} \left[(N_\xi - \rho) \frac{\partial W}{\partial \xi} \right] = 0. \quad (54)$$

with the stretching-bending coupling from

$$N_\xi = 6 \int_0^1 \left(\frac{\partial W}{\partial \xi} \right)^2 d\xi. \quad (55)$$

We can conduct a **single mode analysis** of this system by assuming

$$W(\xi, \tau) = A(\tau) \sin \pi \xi \quad (56)$$

and placing this in equations 54 and 55 we get

$$\ddot{A} \sin \pi \xi + A \pi^4 \sin \pi \xi - (p + 3A^2)(-A \pi^2 \sin \pi \xi) = 0 \quad (57)$$

and thus

$$\ddot{A} + A(\pi^4 - p\pi^2) + 3\pi^2 A^3 = 0. \quad (58)$$

This is a **cubic (hardening) spring oscillator**. Hence we expect to see the stiffening effect due to the immovable ends, even when the deflection is **not** especially large. In the absence of axial load, and for small amplitude motion (such that the cubic term is negligible), we simply have a harmonic oscillation with a frequency of

$$\Omega_n^2 = \pi^4 \quad (59)$$

which in dimensional terms is the familiar first mode (bending) frequency

$$\omega_n = \pi^2 \sqrt{\frac{EI}{mL^4}} \quad (60)$$

Again we can examine the condition $\omega_n^2 \rightarrow 0$ to obtain the critical value of the axial load

$$p = \pi^2 \quad (61)$$

which is, of course, the Euler load

$$P = EI \left(\frac{\pi}{L} \right)^2. \quad (62)$$

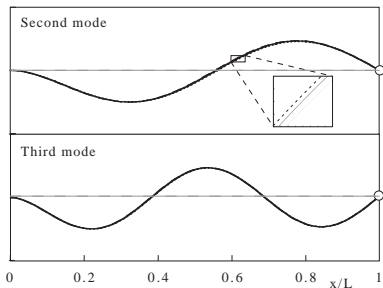
This is the load at which the beam would buckle (assuming no initial imperfections) if slowly increased from zero. Again the linear relation between the axial load and square of the natural frequency is confirmed. The fundamental mode of vibration however, although dominating the motion, would also be accompanied by higher modes (for arbitrary initial conditions), a subject we turn to next.

Although it is the lowest critical load (and its corresponding mode shape) that dominates a typical buckling problem, the higher modes in vibration play a more significant role.

Returning to an earlier example considered (clamped-pinned) we can extract other roots from the characteristic equation (equation 19). The table below shows how the natural frequencies corresponding to higher modes also diminish with axial load:

	$P = 0$	$P = 0.5P_{cr}$	$P = -0.5P_{cr}$
Ω_1	15.42	10.42	19.09
Ω_2	49.94	44.95	54.52
Ω_3	104.25	99.11	109.14

The figure below shows the corresponding mode shapes. Thus we see that despite a relatively strong influence of axial load on natural frequencies, the effect on mode shape is minor (this will not necessarily to the case for more complicated structures like plates and shells).



The second and third modes for a clamped-pinned strut. The inset shows the curves in the presence of tensile and compressive axial forces

For the approximate analysis we return to the simply-supported case and add a **second term** to the assumed shape:

$$W(\xi, \tau) = A_1(\tau) \sin \pi\xi + A_2(\tau) \sin 2\pi\xi \quad (63)$$

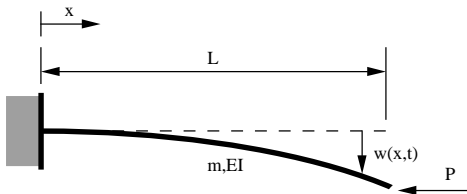
Using equation 63 to evaluate equations 54 and 55 now leads to the pair of equations

$$\ddot{A}_1 + 3\pi^2 A_1(A_1^2 + A_2^2) + A_1(\pi^4 - p\pi^2) = 0 \quad (64)$$

$$\ddot{A}_2 + 12\pi^2 A_2(A_1^2 + A_2^2) + A_2(16\pi^4 - 4p\pi^2) = 0, \quad (65)$$

If we further assume that deflections are small, then we get the second lowest critical load ($p = 4\pi^2$) and a second lowest mode of vibration ($\Omega = 4\pi^4$), both of which correspond to a **full** sine wave. That the linearized equations are uncoupled is a consequence of the assumed modes actually corresponding to the normal modes. For a general structure this will not typically be the case.

Consider a cantilever strut shown below.



Schematic of a cantilevered strut.

In choosing the assumed buckling and vibration modes we wish to have a function that resembles the true modes as closely as possible. Even for a relatively simple structure (like the cantilever under consideration) these modes can be quite complicated. However, it is natural to assume a function which at least satisfies the geometric boundary conditions.

The cubic polynomial

$$w(x, t) = C(t)x^2 + D(t)x^3, \quad (66)$$

satisfies the conditions of zero displacement and slope when $x = 0$. We use this to evaluate the strain energy in bending

$$U = \frac{1}{2} \int_0^L w''^2 dx = 2EIL(C^2 + 3CDL + 3D^2L^2), \quad (67)$$

the potential energy of the end load

$$V_P = -P \frac{1}{2} \int_0^L w'^2 dx = -\frac{PL^3}{30}(20C^2 + 45CDL + 27D^2L^2), \quad (68)$$

and the kinetic energy

$$T = \frac{1}{2} m \int_0^L \dot{w}^2 dx = \frac{m}{210}(21\dot{C}^2L^5 + 35\dot{C}\dot{D}L^6 + 15\dot{D}^2L^7). \quad (69)$$

Again, in the vicinity of equilibrium and for linear vibrations we expect the total potential and kinetic energies to be quadratic functions of the generalized coordinates and velocities respectively, and thus

$$T = \frac{1}{2} T_{ij} \dot{q}_i \dot{q}_j \quad (70)$$

$$U + V_P = \frac{1}{2} V_{ij}^E q_i q_j, \quad (71)$$

where use is made of the dummy suffix notation, i.e., any suffix occurring more than once in a product must be summed over all values.

Evaluating the partial derivatives leads to the second variation of the strain energy:

$$U_{ij} = EIL \begin{bmatrix} 4 & 6L \\ 6L & 12L^2 \end{bmatrix}, \quad (72)$$

the work done by the axial load

$$V_{P_{ij}} = -PL^3 \begin{bmatrix} (4/3) & (3/2)L \\ (3/2)L & (9/5)L^2 \end{bmatrix}, \quad (73)$$

and the kinetic energy

$$T_{ij} = mL^5 \begin{bmatrix} (1/5) & (1/6)L \\ (1/6)L & (1/7)L^2 \end{bmatrix}. \quad (74)$$

We note that these matrices would have been of infinite dimension and diagonal if the exact mode shapes had been used. We next make use of the following definitions

$$\Omega^2 = \frac{mL^4}{EI} \omega^2, \quad \rho = \frac{PL^2}{EI}, \quad (75)$$

and using the characteristic determinantal equation

$$|U_{ij} - V_{P_{ij}} - \omega^2 T_{ij}| = 0 \quad (76)$$

we obtain the characteristic equation

$$12 - 5.2\rho - 0.97\Omega^2 + 0.05\rho\Omega^2 + 0.15\rho^2 + 0.000794\Omega^4 = 0, \quad (77)$$

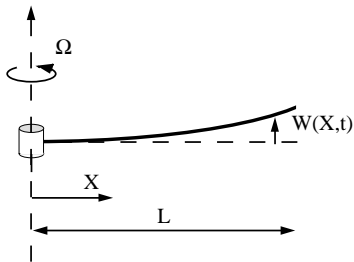
from which we can readily extract the roots.

In the absence of an axial load ($p = 0$), we have a lowest root of $\Omega^2 = 12.6$. This compares with an exact value of 12.36. By setting the natural frequency to zero we obtain a lowest root of $p = 2.49$, which compares with the exact value of $\pi^2/4$. The other roots correspond to the higher of the two modes, although these are less accurate. It is interesting to note that using a single generalized coordinate (e.g., with $D = 0$) leads to a critical load of $p = 3$ and a natural frequency of $\Omega^2 = 20$.

There are a number of ways in which the accuracy of approximate methods can be improved.

Rotating Beams

An example of slender beams subject to tensile axial loads can be found in rotor blades. Centrifugal forces due to high rates of rotation typically lead to stiffening effects. Consider the rotating (cantilever) beam shown below.



A rotating cantilever beam.

We can write the governing equation of motion in the usual form

$$\frac{\partial^2}{\partial x^2} \left(EI \frac{\partial^2 w}{\partial x^2} \right) - \frac{\partial}{\partial x} \left(P \frac{\partial w}{\partial x} \right) + m \frac{\partial^2 w}{\partial t^2} = 0, \quad (78)$$

but now the axial load P (in tension) is given by

$$P = \int_x^L m \Omega^2 x dx. \quad (79)$$

We see that this is similar to equation (13). Separating variables using $w = W(x)Y(t)$, setting the constant equal to $\lambda^2 \Omega^2$, we can write equation (78) (for a uniform beam) in terms of two separated variables

$$EI \frac{d^4 W}{dx^4} - \frac{d}{dx} \left(P \frac{dW}{dx} \right) - m\lambda^2 \Omega^2 W = 0, \quad (80)$$

and

$$\frac{d^2 Y}{dt^2} + \lambda^2 \Omega^2 Y = 0, \quad (81)$$

and scaling using $\bar{w} = W/L$, $\bar{x} = x/L$, and $\psi = \Omega t$, we can then write

$$EI \frac{d^4 \bar{w}}{d\bar{x}^4} - L^2 \frac{d}{d\bar{x}} \left(P \frac{d\bar{w}}{d\bar{x}} \right) - m\lambda^2 \Omega^2 L^4 \bar{w} = 0, \quad (82)$$

and

$$\frac{d^2 Y}{d\psi^2} + \lambda^2 Y = 0. \quad (83)$$

Boundary conditions appropriate for a cantilever beam are zero deflection and slope at the hub (clamped) end and zero bending moment and shear force at the free end. Equation (82) can be attacked in a variety of ways, but it is recognized that since the axial force is not a constant (equation 79) in this case recourse to approximate solution techniques is required. We have already seen the general influence of tensile axial loads on the natural frequencies of lateral vibrations. In applications to rotor blades (e.g., in helicopters and turbines) it is interesting to note that a common configuration is to use a hinge at the root of the beam, and hence the somewhat unusual boundary conditions of pinned-free are encountered. In this case the lowest mode is a rigid body rotation (a **flapping motion**). The cantilever is often termed a **hingeless blade**.

Here, we briefly mention a useful approach (related to Rayleigh-Ritz) due to **Southwell**. He showed that a relation between the rotating and non-rotating frequencies could be established as

$$\omega_i^2 = \omega_{nr}^2 + \alpha_i \Omega^2, \quad (84)$$

where ω_{nr} is the natural frequency of the non-rotating blade and the Southwell coefficient α_i is given by

$$\alpha_i = \frac{\int_0^1 m\bar{x} [\int_0^{\bar{x}} (d\bar{w}_i/d\bar{x})^2 d\bar{x}] d\bar{x}}{\int_0^1 m\bar{w}_i^2 d\bar{x}}, \quad (85)$$

and where $\bar{w}_i = \bar{w}_i(x)$ is an assumed mode shape, satisfying the boundary conditions. Although α_i is not strictly constant, the mode shape changes very little with rotation speed.

For $\Omega \rightarrow 0$ we get the lowest bending mode, which for a pinned-free cantilever is $15.418\sqrt{EI/(mL^4)}$, and for a clamped-free cantilever is $3.516\sqrt{EI/(mL^4)}$. As the rate of rotation gets large we observe an asymptotic relation $\omega_i \rightarrow \sqrt{\alpha_i}\Omega$.

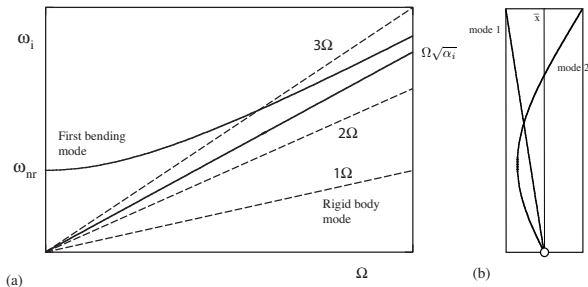
For example

$$\gamma = c_1\gamma_1 + c_2\gamma_2, \quad (86)$$

in which

$$\gamma_1(x) = x, \quad \gamma_2(x) = 10x^3/3 - 10x^4/3 + x^5. \quad (87)$$

It is shown that the two roots resulting from this analysis correspond to the frequencies $\omega = \Omega$ (flapping motion) and $\omega = 2.757\Omega$, and the (normalized) mode shapes plotted:



(a) A 'spoke' diagram showing the relation between natural frequencies and rate of rotation, (b) The first two mode shapes of a pinned-free rotating beam using an assumed solution (Bramwell).

Given this basic shape, use can be made of Southwell's method (equation 85), to show how the frequencies change with the speed of rotation according to part (a).

Here, we show the table below which summarizes the effect of rotation rate on the lowest three frequencies of clamped-free and pinned-free uniform cantilevers in which $\eta = \Omega/\sqrt{EI/mL^4}$:

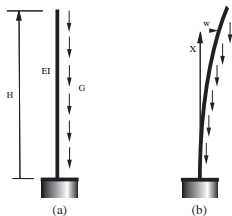
η		Clamped-free	Pinned-free
0	ω_1	3.5160	0.000
	ω_2	22.0345	15.4182
	ω_3	61.6972	49.9649
1	ω_1	3.6816	1.000
	ω_2	22.1810	15.6242
	ω_3	61.8418	50.1437
3	ω_1	4.7973	3.000
	ω_2	23.3203	17.1807
	ω_3	62.9850	51.5498

A considerable amount of research has been conducted on **modal interaction** in rotor blades due to elastic and inertial coupling. Clearly, the effects of fluid loading (including forward flight) is complicated, but suffice it to say here that there are practical situations in which there is elastic coupling between flapping and lagging motion. Southwell's method can be applied and flap-lag dynamic interaction obtained. This is an important design consideration for helicopters and stability boundaries have been developed to take into account the various parameters of the problem. Given the periodic nature of rotating systems certain special mathematical techniques can be employed including **Floquet theory**.

Turbomachinery tends to operate at extremely high rates of revolution and their blades can experience considerable stiffening effects. For example, tip speeds can be close to Mach 1, i.e., a small turbine with a radius of a few centimeters might operate at 100,000 rpm, whereas a large commercial jet engine might operate in the vicinity of 1,500 rpm. Use is made of **Campbell diagrams** (also known as **waterfall plots** and **spectrograms**) to keep the natural frequencies away from the harmonics of the rotor speed. Circular plates are sometimes designed so that their natural frequencies can be tuned as a function of the rate of spinning.

Self-weight

Consider the column shown below



Geometry of column subjected to self-weight.

It has height H , constant bending stiffness EI , and constant weight W per unit length. We would expect this column to buckle under its own weight at a critical height, followed by a gradual droop corresponding to a stable-symmetric (or super-critical) bifurcation. Again, we would also expect the lowest natural frequency to reduce with axial load (column height).

The equilibrium equation is

$$EIY''''(X) + W [(H - X)Y'(X)]' = 0. \quad (88)$$

To put the analysis in nondimensional terms, define

$$a = \left(\frac{EI}{W} \right)^{1/3}, \quad x = \frac{X}{a}, \quad y = \frac{Y}{a}, \quad h = \frac{H}{a}. \quad (89)$$

(The lengths are not nondimensionalized by H, since the height is the parameter of interest.) This leads to the following equation:

$$y''''(x) + [(h - x)y'(x)]' = 0. \quad (90)$$

The boundary conditions are $y(0) = y'(0) = y''(h) = y'''(h) = 0$. The critical nondimensional height is $h_{cr} = 1.986$.

Approximate values of the critical height can be obtained with the use of the Rayleigh-Ritz method as described earlier. The potential energy U is given by

$$U = \frac{1}{2} \int_0^h (y'')^2 dx - \frac{1}{2} \int_0^h (h-x)(y')^2 dx. \quad (91)$$

Making U stationary for the kinematically-admissible function

$$y(x) = Qx^c \quad (92)$$

where $c > 1$ leads to the approximate critical height $h_{cr} = 2.289$ if $c = 2$, and the value $h_{cr} = 2.143$ for the minimizing choice $c = 1.747$. If

$$y(x) = Q[1 - \cos(cx/h)], \quad (93)$$

one obtains $h_{cr} = 2.025$ for $c = \pi/2$ (corresponding to the buckling mode for a cantilever with axial end load), and $h_{cr} = 2.003$ for the optimal value $c = 1.829$. Finally, the two-term approximation

$$y(x) = Q_1x^2 + Q_2x^3 \quad (94)$$

furnishes the excellent approximation $h_{cr} = 1.991$.

For a **circular cross section** of radius R we can also use a Rayleigh-Ritz analysis (based on a simple polynomial displacement function) to obtain **critical height** for uniform pole:

$$h_c = 1.26 \left(\frac{E}{\rho} R^2 \right)^{1/3}, \quad (95)$$

in which ρ is the specific weight. For a uniform taper ($r = (h - x)R_0/h$) in which R_0 is the radius at the base of the cantilever the coefficient in equation 95 changes to 2.17. It is interesting to note that a rule of taper appropriate for trees ($r = ((h - x)/h)^{3/2}R_0$) the coefficient becomes 2.60 so we see a somewhat optimal design in nature (at least in terms of vertical loading).

A Hanging Beam

A related problem to self-weight buckling is the behavior of long vertical pipes which are subject to axial loads which are not uniform and might, for example, be due to the combined effects of gravity and hydrostatic pressure. A practical example would be the behavior of drill strings in a well bore. Again various end conditions are possible but we shall focus attention on the specific case of a vertical beam, fully fixed at its top end and completely free at the bottom. Hydrostatic pressure is assumed to vary linearly with distance from the top, i.e., a submerged column, and the effect of gravity is included in the following analysis. At the end of this section we will show that for very long and slender beams the behavior tends towards that of the hanging chain encountered earlier.

The governing equation of motion is based on the usual assumptions of linearly elastic material and small deflections, and hence we still have equation (1) with an additional term:

$$EI \frac{\partial^4 w}{\partial x^4} - \frac{\partial}{\partial x} \left[(w - w_m) x \frac{\partial w}{\partial x} \right] + m \frac{\partial^2 w}{\partial t^2} = 0. \quad (96)$$

Again we assume harmonic motion of the form $w = W(x) \sin \omega t$ and thus

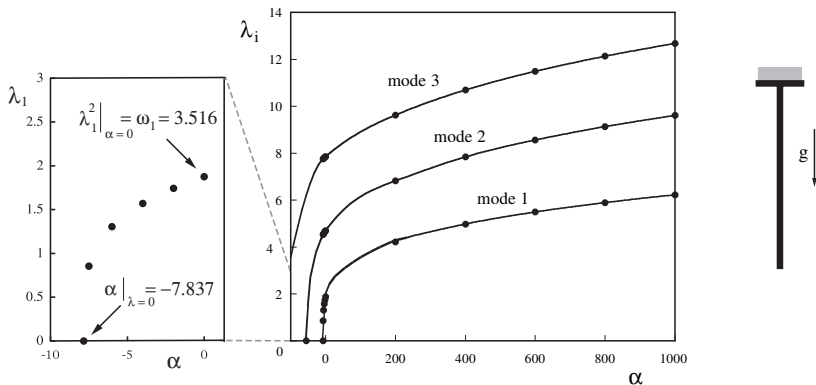
$$\frac{d^4 W}{d\zeta^4} - \alpha \zeta \frac{d^2 W}{d\zeta^2} - \alpha \frac{dW}{d\zeta} - \lambda^4 W = 0, \quad (97)$$

in which

$$\lambda^4 = m\omega^2 L^4 / (EI), \quad \alpha = (w - w_m) L^3 / (EI), \quad \zeta = x/L. \quad (98)$$

In the above expressions m is the mass per unit length, L is the length of the pipe, x is the distance from the lower end, W is the weight per unit length, w_m is the weight of the fluid displaced by the pipe, and ω is the natural frequency of the motion. In the following analysis the parameter α (in which the component $(w - w_m)$ can be thought of as the **traction**) will be set, and a solution given for λ .

For the specific case under consideration the boundary conditions consist of fixed at the top end: $W(1) = dW/d\zeta(1) = 0$, and free at the lower end: $d^2W/d\zeta^2(0) = d^3W/d\zeta^3(0) = 0$. The figure below shows the three lowest frequencies as a function of α .

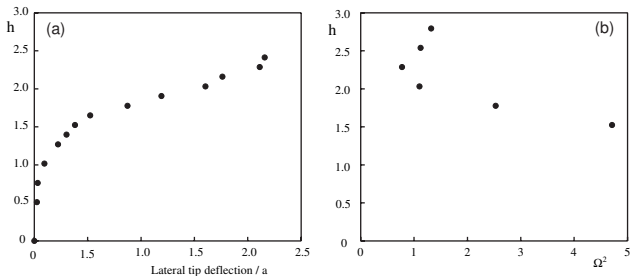


Natural frequencies of a hanging beam as a function of α (Huang and Dareing).

It can be shown that the lowest natural frequency (mode 1) drops to zero when the traction reaches a level of $\alpha = -7.8373$, i.e., buckling occurs. In the case of a hanging beam with no hydrostatic pressure but under the action of gravity alone we can effectively reduce the bending stiffness of the system by allowing α to go to very large values, i.e., very large tensions. This tends towards the behavior of a hanging chain, e.g., with $\alpha = 1000$ we get a lowest natural frequency coefficient tends to 1.22. This compares with the hanging chain value of 1.2026 which would have been even more closely matched if the upper support were pinned rather than fixed.

Experiments

A cantilever under the action of self-weight loading provides a relatively simple context for experimental verification of some of the behavior described in this section. Consider first a vertically-mounted (built-in end at the bottom), slender elastic rod, of axisymmetric (circular) cross-section, whose length can be increased such that (self-weight) buckling is induced. A cantilever test was conducted whilst the beam was mounted in a horizontal configuration to determine the flexural rigidity, and this estimate suggested a critical elastic buckling length in the vicinity of 20 cm, based on $1.986(EI/W)^{1/3}$. The lateral deflection was measured as a function of height and the results plotted in part (a) of the next slide. The **supercritical** nature of the bifurcation is apparent. In part (b) of this figure the lowest natural frequency is also plotted as a function of height. The minimum is achieved in the vicinity of the critical height: it does not drop to zero in practice because of the inevitable presence of a geometric imperfection (in fact for this type of axisymmetric cross section there is no obvious preferred direction for postbuckled deflection in the perfect case).

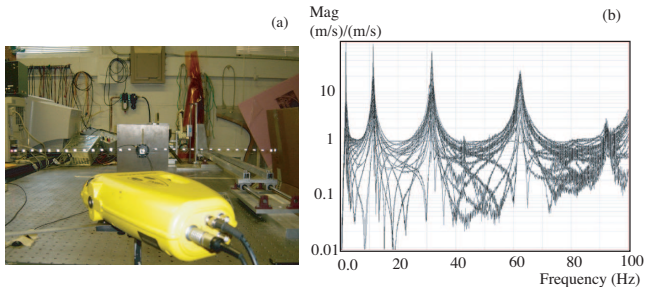


(a) Tip deflection and (b) fundamental frequency for a slender rod.

Also, frequencies become increasingly difficult to measure (for small amplitude vibration) near the buckling length due to the increasing effect of damping. It can also be argued that the damping force has less effect because the velocities are decreasing. The postbuckled equilibria and frequencies (which start to increase in the postbuckling range) can be studied in the context of an **elastica** analysis.

Another method of illustrating the effect of gravity is to conduct tests on a **double** cantilever, i.e., a thin rod clamped at its center point and oriented in the vertical direction. As the rod becomes more slender, the difference between the **upright** and **downward** natural frequencies becomes more apparent. A number of thin polycarbonate strips were fabricated such that a range of the nondimensional parameter α (see equation 98) could be examined. The hub was clamped to an electro-magnetic shaker and the system subject to a broadband, random excitation. A laser vibrometer was then used to acquire velocity data from discrete locations along both beams, and subsequent signal processing used to obtain frequency response data.

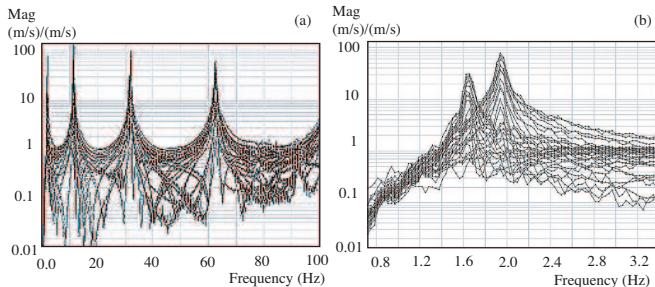
Consider a **horizontal** polycarbonate strip with cross-sectional dimensions of 25.4×4.67 mm, Young's modulus $E = 1.93$ GPa, mass per unit length $m = 0.131$ kg/m, and length $L = 0.737$ m.



A thin prismatic cantilever, (a) experimental configuration, (b) frequency response.

Part (b) showing the superimposed frequency response extracted from 30 evenly spaced locations along the entire length. The four lowest measured natural frequencies (in Hz) are 1.812, 11.34, 31.71 and 62.35, which compare with analytical values (based on equation 96) of 1.836, 11.51, 32.22 and 63.13.

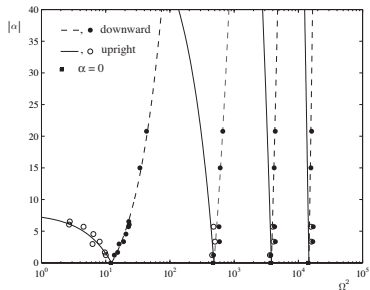
Now, if we take the same system and rotate it 90 degrees we get the frequency separation (**mode splitting**) shown below:



Normalized frequency response spectrum for a cantilever in a gravitational field, $|\alpha| = 1.23$ (a) lowest few frequencies, (b) blow-up of the lowest frequency.

Upon closer inspection each peak is revealed as **two** adjacent peaks. For larger values of α the up or down orientation has a greater effect. For example, when we reduce the thickness of the strip to 2.38 mm, and the length to 0.66 m, while holding everything else constant, we then have $|\alpha| = 5.71$, and the two peaks separate to approximately 1.65Hz and 1.95Hz.

For the upright cantilever we have the result that buckling occurs when $\alpha = -7.837$, and the trivial equilibrium loses its stability. Thus, the results just shown (for which $|\alpha| = 1.23$) correspond to a cantilever whose length is $(1.23/7.837)^{1/3} = 55\%$ of its buckling length. We show the results graphically below for both analytical and experimental frequencies versus α . The lowest frequency, as expected, drops to zero when $|\alpha| = -7.837$.



The four lowest frequencies vs. $|\alpha|$.

Thermal Loading

We briefly consider the situation in which the axially load is produced through a **thermal gradient**. We start by looking at a simply-supported beam which is not allowed to move axially at its ends (and thus generating axial forces). If the beam, with coefficient of linear thermal expansion α is subject to a constant thermal load, the governing equation of motion becomes

$$m\ddot{w} + EIw^{IV} + AE(\alpha T)w'' = 0, \quad (99)$$

and thus we obtain a natural frequency which is a function of the temperature change:

$$\omega^2 = \left(\frac{\pi}{L}\right)^4 \left(\frac{EI}{m}\right) \left[1 - (\alpha T) \left(\frac{L}{\rho\pi}\right)^2\right] \quad (100)$$

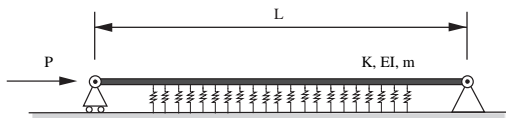
where $\rho = \sqrt{I/A}$ is the radius of gyration.

In the absence of a temperature gradient we recover the natural frequency of a regular simply-supported beam. Again we have a natural frequency that drops to zero as the critical buckling temperature is approached, but increases if the beam is cooled:

$$T_{cr} = \left(\frac{\rho\pi}{L}\right)^2 \frac{1}{\alpha} \quad (101)$$

Of course, this solution depends on the ends of the beam being prevented from moving, but we basically obtain Euler buckling. The issue of thermal loading is a very complicated one especially for non-simple structures and non-uniform heating.

Beam on an Elastic Foundation



A schematic of a thin elastic beam restrained by a linearly elastic foundation.

It is not uncommon for a beam to have some kind of **continuous support** along its length. We can think of this as an elastic foundation, and assume the foundation stiffness is linear. A practical example of this might be the sleepers under a railroad track, where a significant axial loading effect is caused by thermal expansion. Referring to the schematic shown in the above figure, and again assuming the ends of the beam are pinned, we can extend the analysis from earlier.

The incorporation of a linear elastic foundation results in additional strain energy stored in the foundation

$$U_K = \frac{1}{2}K \int_0^L w^2 dx \quad (102)$$

$$= \frac{1}{2}K \int_0^L q_i^2 \sin^2 \frac{i\pi x}{L} dx \quad (103)$$

$$= \frac{1}{2}Kq_i^2 \frac{L}{2}. \quad (104)$$

Therefore, we obtain the natural frequencies

$$\omega_i^2 = \frac{1}{m} \left[EI \left(\frac{i\pi}{L} \right)^4 + K - P \left(\frac{i\pi}{L} \right)^2 \right]. \quad (105)$$

Clearly we recover the results from earlier when we set $K = 0$, but depending on the stiffness of the elastic foundation we see the possibility of a frequency **other** than the first (corresponding to a half sine wave) dropping to zero first under the action of increasing P .

Introducing the following nondimensional parameters

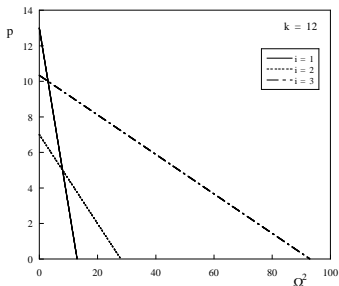
$$\Omega^2 = \frac{\omega^2}{\frac{EI}{m} \left(\frac{\pi}{L}\right)^4}, \quad p = \frac{P}{EI \left(\frac{\pi}{L}\right)^2}, \quad k = \frac{K}{EI \left(\frac{\pi}{L}\right)^4}, \quad (106)$$

we obtain nondimensional equations for each mode

$$\begin{aligned} 1 + k - p &= \Omega^2 & : i = 1, \\ 16 + k - 4p &= \Omega^2 & : i = 2, \\ 81 + k - 9p &= \Omega^2 & : i = 3, \end{aligned} \quad (107)$$

and so on. Without the elastic foundation we observe the familiar relation between the axial load and the square of the natural frequency. However, the elastic foundation has an interesting effect on the critical loads, e.g., we see that when $k = 4$ the lowest two buckling loads are the same ($p = 5$). For $4 < k < 36$, the critical value of p is $4 + (k/4)$ and the corresponding mode has two half-sine waves. In general, if $(n-1)^2 n^2 < k < n^2 (n+1)^2$, the critical value of p is $n^2 + k/(n)^2$ and the governing buckling mode has n half-sine modes.

Suppose we fix $k = 12$. The relationships in equations (107) are plotted below:



The interaction of axial load and natural frequencies for a pinned beam resting on a foundation with stiffness $k = 12$.

For this specific foundation stiffness we have (in the absence of axial loads) frequencies $\Omega_1^2 = 13$, $\Omega_2^2 = 28$, $\Omega_3^2 = 93$. The lowest three buckling loads (i.e., when the lowest natural frequency is zero) are $p_2 = 7$, $p_3 = 10.33$, $p_1 = 13$. We see how these modes have **changed order**.

Elastically Restrained Supports

It may happen that the actual boundary conditions do not correspond exactly to the classification of pinned, fixed, etc. In this case elastic springs can be incorporated into the analysis such that when the torsional stiffness is set equal to zero we obtain the pinned or simply-supported case, and when it is infinite we have the fully fixed boundary condition. This allows for a range of intermediate values that can be used to reflect varying degrees of partial restraint.

Since the elastic end constraints only affect the boundary conditions we still have the familiar equation governing the small amplitude, harmonic, transverse vibrations of a beam given by

$$\frac{d^4 W}{dx^4} + p \frac{d^2 W}{dx^2} - \Omega^2 W = 0, \quad (108)$$

in which

$$W = w/L, \quad \bar{x} = x/L, \quad p = PL^2/EI, \quad \Omega^2 = \rho A \omega^2 L^4/EI. \quad (109)$$

Again, the solution is given by

$$W = C_1 \sinh \alpha \bar{x} + C_2 \cosh \alpha \bar{x} + C_3 \sin \beta \bar{x} + C_4 \cos \beta \bar{x}, \quad (110)$$

with

$$\begin{aligned} \alpha^2 &= \sqrt{(p^2/4) + \Omega^2} + p/2 \\ \beta^2 &= \sqrt{(p^2/4) + \Omega^2} - p/2. \end{aligned} \quad (111)$$

Note the similarity between equations (111) and (15), with the slight difference due to the definition of nondimensional load used in equation (16) compared with equation (109).

However, with torsional end constraint the boundary conditions become

$$\begin{aligned} W(0) &= W(1) = 0 \\ d^2W/d\bar{x}^2 - \sigma_1 dW/d\bar{x} &= 0 \quad \text{at} \quad \bar{x} = 0 \\ d^2W/d\bar{x}^2 + \sigma_2 dW/d\bar{x} &= 0 \quad \text{at} \quad \bar{x} = 1 \end{aligned} \quad (112)$$

where

$$\sigma_1 = k_1L/EI, \quad \sigma_2 = k_2L/EI, \quad (113)$$

and the k 's are the spring stiffness at the left and right hand ends, respectively.

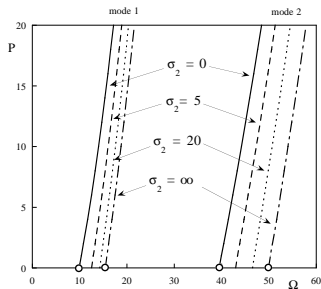
Application of the above conditions leads to the characteristic equation

$$[(\alpha^2 + \beta^2)^2 + \sigma_1\sigma_2(\alpha^2 - \beta^2)] \sinh \alpha \sin \beta - \quad (114)$$

$$2\sigma_1\sigma_2\alpha\beta(\cosh \alpha \cos \beta - 1)$$

$$+(\sigma_1 + \sigma_2)(\alpha^2 + \beta^2)(\alpha \cosh \alpha \sin \beta - \beta \sinh \alpha \cos \beta) = 0. \quad (115)$$

We consider a specific case of a beam, subject to a tensile axial force, with the left-hand end pinned ($\sigma_1 = 0$), and the right-hand end subject to a torsional spring (σ_2). Thus we can examine the dynamics of the beam ranging from zero end rotational stiffness (i.e., a pinned-pinned beam) to infinite end rotational stiffness (i.e., a pinned-clamped beam), to compare with some of the previous results. The figure shows how the lowest two natural frequencies vary with tensile axial load for different levels of end torsional restraint.

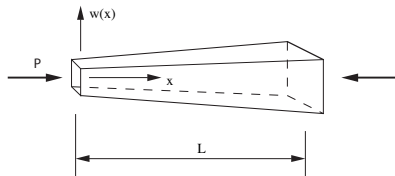


Variation of the lowest two natural frequencies with tensile axial load for varying end constraint.

For zero axial load we observe the frequency coefficients $\Omega_1 = \pi^2$ and $\Omega_2 = 4\pi^2$ for the pinned-pinned case (i.e., $\sigma_2 = 0$). The natural frequencies increase with tensile force as expected. For pinned-fixed boundary conditions ($\sigma_2 = \infty$) we obtain the frequencies $\Omega_1 = 15.4$ and $\Omega_2 = 50.0$. These cases are indicated by the circles. Two intermediate cases are also shown: for $\sigma_2 = 5$ and $\sigma_2 = 20$. In those cases in which a structural component makes up one element of a larger structure, or framework, then the actual boundary conditions will typically depend on the stiffness provided by adjacent members, and this will be the focus later, when we consider frames.

Beams with Variable Cross-section

In this section we make use of the Rayleigh-Ritz approach to obtain the axial load versus frequency relation for a simply supported beam with a square cross section ($h \times h$) and a linear taper as shown below:



A schematic of a thin elastic beam whose size is a linear function of its length.

The column length is L , Young's modulus E , and density ρ . The width (and depth) at any distance x along the length of the column is given by

$$h(x) = h(0) \left[1 + \frac{\alpha - 1}{L} x \right], \quad (116)$$

in which $\alpha = h(0)/h(L)$.

From this, we can compute the area and second moment of area:

$$\begin{aligned} A(x) &= A(0) [1 + x(\alpha - 1)/L]^2 \\ I(x) &= I(0) [1 + x(\alpha - 1)/L]^4, \end{aligned} \quad (117)$$

where $A(0) = h(0)^2$ and $I(0) = h(0)^4/12$ are the area and second moment of area at the left hand (smaller) end. Given simply-supported boundary conditions we can assume a half sine wave as the fundamental mode (we know this is exact for a prismatic beam), i.e., $w(x) = C \sin \pi x/L$. The energy expressions for strain energy in bending, potential energy of the loading, and kinetic energy are given by

$$U = \frac{1}{2} \int_0^L EI(x) w''^2 dx \quad (118)$$

$$V_P = \frac{1}{2} \int_0^L P w'^2 dx \quad (119)$$

$$T = \frac{1}{2} \int_0^L \rho A(x) \dot{w}^2 dx. \quad (120)$$

These expressions can be evaluated for the assumed mode shape which results in

$$U = \frac{1}{4}EI(0)LC^2 \left(\frac{\pi}{L}\right)^4 \left[1 + 2(\alpha - 1) + (2 - 3/\pi^2)(\alpha - 1)^2 + (1 - 3/\pi^2)(\alpha - 1)^3 + (1/5 - 1/\pi^2 + 3/(2\pi^4))(\alpha - 1)^4 \right] \quad (121)$$

$$V_P = \frac{1}{4}LPC^2 \left(\frac{\pi}{L}\right)^2 \quad (122)$$

$$T = \frac{1}{4}L\rho A(0)\dot{C}^2 [1 + (\alpha - 1) + (1/3 - 1/(2\pi^2))(\alpha - 1)^2] . \quad (123)$$

We can then make use of Lagrange's equation or Rayleigh's method to obtain the natural frequency in the usual way.

We note that this result subsumes the case of a prismatic (constant cross section) beam in which $\alpha = 1$. However, in general we get

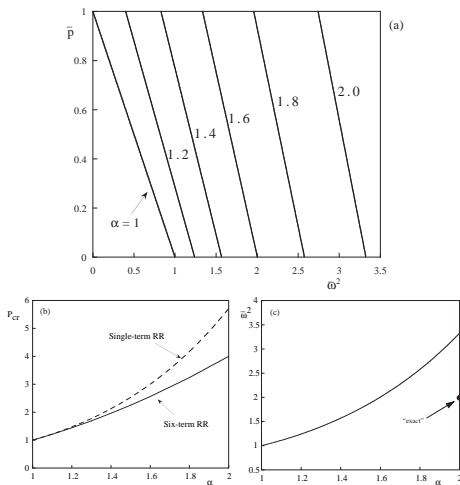
$$\bar{\omega}^2 = \frac{[1 + 2(\alpha - 1) + 1.696(\alpha - 1)^2 + 0.696(\alpha - 1)^3 + 0.317(\alpha - 1)^4 - \bar{p}]}{[1 + (\alpha - 1) - 0.283(\alpha - 1)^2]}, \quad (124)$$

where the natural frequency and axial load are nondimensionalized according to

$$\bar{\omega}^2 = \frac{\omega^2}{EI(0)/m(\frac{\pi}{L})^4} \quad \bar{p} = \frac{P}{EI(0)(\frac{\pi}{L})^2}. \quad (125)$$

For the prismatic beam ($\alpha = 1$), we get the exact coefficients from earlier.

The effect of a varying cross section is shown on the next page. The linearity of the \bar{p} vs $\bar{\omega}^2$ relation in part (a) is a consequence of the single-mode assumption. By increasing the value of α we are stiffening the beam, and hence both the critical load and natural frequency increase. For example for a beam whose cross-sectional dimension at $x = L$ is twice that at $x = 0$, i.e., $\alpha = 2$ results in a nondimensional critical load of approximately 5.47, and a natural frequency (squared) in the absence of axial load of about 3.3.



(a) The frequency-load relation for various tapered columns; (b) variation of the critical load with taper (with a sample 'exact' result for $\alpha = 2$ superimposed), (c) variation of natural frequency with taper, when the axial load is zero.

The variable cross section does, of course, render the sine wave an approximate mode shape. More terms in the Rayleigh-Ritz procedure can be used. The result of using (a very accurate) six terms in just such an expansion is also shown in the figure as an isolated data point, and specifically for $\alpha = 2$ in part (c). As the degree of taper increases the single-mode approximation breaks down.

The analysis is simplified somewhat if it is assumed that it is the second moment of area that varies linearly with length rather than the cross-sectional dimension, or if a beam is a wedged shape then the area will vary linearly with length and the second moment of area will vary as the cube of the length, and so on. Tapered columns which are loaded by their self-weight can also be handled, although the mass distribution must also be taken into account. Of course, the **height to which a tree might grow** is a nice example of this, although it is the lateral loading caused by wind that ultimately limits height. It has been shown that many trees have a **natural taper** of the form

$$R = R(0) \left[\frac{h-x}{h} \right]^{3/2}, \quad (126)$$

where R is the radius, $R(0)$ the radius at the base, and h is the height. That is, not dissimilar to the profile of the Eiffel tower. **Stepped columns** that have discrete changes in their cross-sectional properties can also be handled in this manner.